Title

Trans-complementation by the RecB nuclease domain of RecBCD enzyme reveals new insight into RecA loading upon χ recognition

Permalink

https://escholarship.org/uc/item/9375q06w

Journal

Nucleic Acids Research, 52(5)

ISSN

0305-1048

Authors

Pavankumar, Theetha L

Wong, C Jason

Wong, Yun Ka

et al.

Publication Date

2024-03-21

DOI

10.1093/nar/gkae007

Copyright Information

Peer reviewed

Trans-complementation by the RecB nuclease domain of RecBCD enzyme reveals new insight into RecA loading upon χ recognition

Theetha L. Pavankumar [1,2,†], C. Jason Wong[1,2,†], Yun Ka Wong[1,2], Maria Spies[3] and Stephen C. Kowalczykowski [1,2,*]

[1]Department of Microbiology and Molecular Genetics, University of California, Davis, CA 95616, USA
[2]Department of Molecular and Cellular Biology, University of California, Davis, CA 95616, USA
[3]Department of Biochemistry, University of Iowa, Carver College of Medicine, Iowa City, IA 52242, USA

[*]To whom correspondence should be addressed. Tel: +1 530 752 5938; Email: sckowalczykowski@ucdavis.edu
[†]The first two authors should be regarded as Joint First Authors.
Present address: Yun Ka Wong, Cancer and Stem Cell Biology Program, Duke-NUS Medical School, Singapore 169857, Singapore.

Abstract

The loading of RecA onto ssDNA by RecBCD is an essential step of RecBCD-mediated homologous recombination. RecBCD facilitates RecA-loading onto ssDNA in a χ-dependent manner via its RecB nuclease domain (RecB^n). Before recognition of χ, RecB^n is sequestered through interactions with RecBCD. It was proposed that upon χ-recognition, RecB^n undocks, allowing RecB^n to swing out via a contiguous 70 amino acid linker to reveal the RecA-loading surface, and then recruit and load RecA onto ssDNA. We tested this hypothesis by examining the interactions between RecB^n (RecB$^{928–1180}$) and truncated RecBCD (RecB$^{1–927}$CD) lacking the nuclease domain. The reconstituted complex of RecB$^{1–927}$CD and RecB^n is functional *in vitro* and *in vivo*. Our results indicate that despite being covalently severed from RecB$^{1–927}$CD, RecB^n can still load RecA onto ssDNA, establishing that RecB^n does not function while only remaining tethered to the RecBCD complex via the linker. Instead, RecBCD undergoes a χ-induced intramolecular rearrangement to reveal the RecA-loading surface.

Graphical abstract
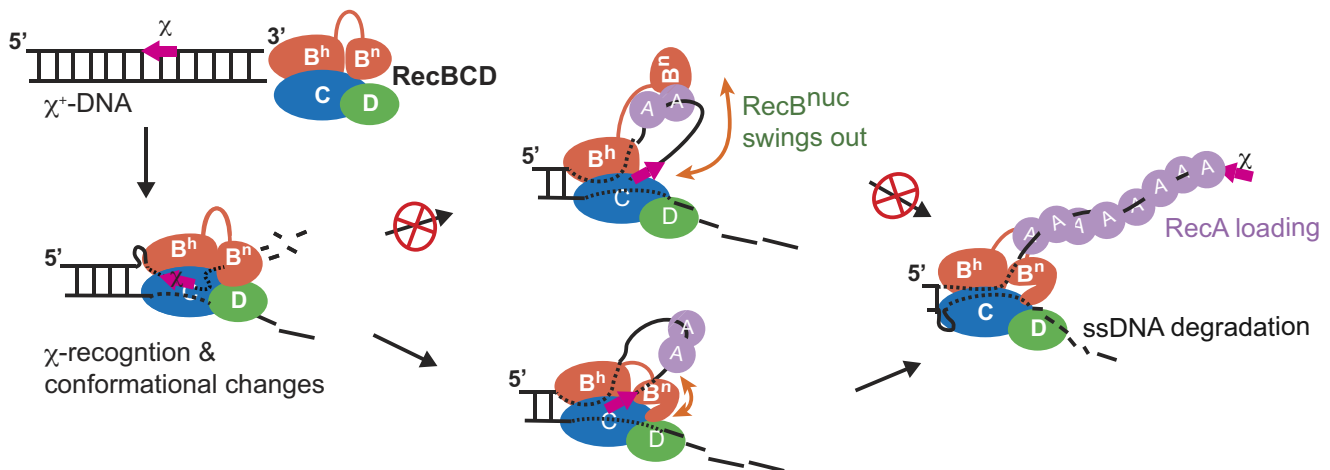
Introduction

The repair of double-stranded DNA (dsDNA) breaks in wild-type *Escherichia coli* requires the functions of RecA and RecBCD proteins (1,2). RecBCD is a heterotrimeric enzyme consisting of RecB, RecC, and RecD subunits (3,4). In its constitutive state, it binds and unwinds from the broken dsDNA ends and simultaneously degrades the 3′-terminated strand at the entry site more extensively than the 5′-terminated strand (5,6). However, the polarity and intensity of nuclease activity is reversed when RecBCD encounters a Chi (χ) sequence (5′-GCTCGTGG-3′) (7–10). The stable binding of χ to the RecC subunit of RecBCD is suggested to prevent the χ-containing ssDNA from passing through the nuclease domain and possibly redirecting it through an alternative exit, resulting in preservation of 3′-ended χ-containing ssDNA (11). RecBCD then facilitates RecA nucleofilament formation by loading

RecA onto the χ-containing ssDNA (12). The RecA nucleofilament subsequently searches for homologous DNA to promote DNA pairing (13). Subsequent maturation of recombination intermediates ensues to complete the repair process (2).

The RecB subunit has two domains with distinct functions: a 100 kDa N-terminal helicase domain (RecB$^{1-927}$; hereafter referred to as RecB^h) and a 30 kDa C-terminal nuclease domain (RecB$^{928-1180}$; hereafter referred to as RecB^n), connected by a 70 amino acid (aa) linker region (residues 858–927 of RecB) serving as a covalent tether between the two structural domains (3,14). The 70 aa linker region is important for RecBCD activities (14,15). Deletion of RecB^n from RecBCD results in a mutant enzyme that fails to load RecA after χ-recognition, suggesting that RecB^n plays an important role in RecA-loading (16); moreover, RecB^n physically interacts with RecA and the areas of RecB^n that can interact with the RecA core region were tentatively identified by computational modeling (17).

Prior to recognition of χ, RecBCD does not interact with RecA and the surface of RecB^n proposed to interact with RecA is buried by interaction with the RecC subunit (3,16,17). However, several studies indicate that the buried RecA-interacting region of RecB^n is revealed upon recognition of χ to facilitate RecA-loading (16–18). The discovery that RecB^{h}CD has helicase activity but no nuclease actively led to the proposal—the 'nuclease domain swing model' (Figure 1A)—that upon χ-recognition, RecB^n can swing away via its tether to elicit many of the changes occurring upon χ-recognition (14). Another potential consequence of this tethered undocking would be exposure of the RecA-interacting region for subsequent RecA-loading (4,15–17).

Despite the prominence and value of the nuclease domain swing model, there are no studies showing that RecB^n is released upon χ-recognition and that the tether plays the important function of maintaining the RecA-loading domain within proximity of the χ-containing ssDNA. If the model is correct, then a RecBCD enzyme with a severed tether should lose RecB^n at χ, and loading of RecA would not ensue (Figure 1B). Here, we show that a functional RecBCD with a severed tether can be reconstituted from a truncated mutant of RecBCD (RecB$^{1-927}$CD) lacking the nuclease domain and a separated RecB nuclease domain (RecB$^{928-1180}$): the severed reconstituted RecBCD complex contains all the residue of the wild-type enzyme but lacks a single peptide bond between amino acid residues 927 and 928. The resulting RecB^{h}CD–RecB^n complex responds to χ sequences, generates χ-containing ssDNA, and loads RecA onto the χ-containing ssDNA. *In vivo*, RecB$^{1-927}$CD and RecB$^{928-1180}$ complement one another to reconstitute nuclease activity, repair UV-damaged DNA and promote χ-dependent recombination. Based on our results obtained from both genetic and biochemical analyses of RecB^{h}CD–RecB^n complex, we conclude that covalent tethering is not required for RecBCD functions, implying that RecB^n does not function at the free end of a flexible linker. Rather, we conclude that the RecA-interaction site of RecB^n is revealed through χ-induced conformational changes within the holoenzyme. We believe that the linker region plays an important role in RecBCD heterotrimer stability and it may serve to ensure the association of RecB^n with the helicase machinery of RecBCD.

Materials and methods

Bacterial strains and phages

The following *Escherichia coli* strains were used in the experiments as described in the method details. AB1157 cells as wildtype, the *recCBD* operon deleted AB1157 (Δ*recCBD::FRT*), V330 (Δ *(recC-argA) 234 λ⁻ F⁻*) (19), 594 (*lac-3350 galK2 galT22 rpsL179 λ⁻ F⁻*), and C600 (*thr-1 leuB6 thi-1 lacY1 tonA21 supE44 rfbD1 λ⁻ F⁻*) (20). The following phage strains were also used in the study. λ 1081 (*susJ6 b1453 cI857 χ⁺D123*), λ 1082 (*b1453 χ⁺D123 susR5*), λ 1083 (*susJ6 b1453 χ⁺76 cI857*), λ 1084 (*b1453 χ⁺76 susR5*), T4 phage (*gene 2⁺*), and T4 2⁻ (*gene 2 amN51*). All the phages were generous gifts from Gerald R. Smith (20).

Reagents and DNA substrates

All the reagents used in this study were of a reagent grade. The reagents are ATP disodium (Cytiva, USA), Adenosine 5′-O-(3-Thiotriphosphate), Tetralithium Salt (ATPγS) (Millipore Sigma, USA), ATP, [γ-^{32}P] 6000 Ci/mmol 10 mCi/ml EasyTide, 250 μCi (PerkinElmer, USA), Phosphoenolpyruvate, Proteinase K (Roche, USA), Ni-NTA Magnetic Agarose Beads (QIAGEN, USA), and Bio-Spin® Columns, Bio-Gel® *P*-30 (BIO-RAD). The ampicillin sodium salt, chloramphenicol, streptomycin dihydrochloride pentahydrate, kanamycin sulfate, L-lactic dehydrogenase and pyruvate kinase were purchased from the Sigma-Aldrich company. The USB® Shrimp alkaline phosphatase was purchased from Affymetrix. Enzymes such as T4 Polynucleotide Kinase (T4 PNK), Klenow Fragment (3′ – 5′, exo⁻), EcoRI-HF, NcoI, NdeI, SexAI and XbaI were purchased from New England Biolabs (NEB, Ipswich, MA). Buffers were made from reagent grade chemicals with Milli-Q water. ATP (Cytiva, USA) and ATPγS (Millipore Sigma, USA) stocks were adjusted to pH 7.5, and concentration was determined spectrophotometrically using $\varepsilon_{260} = 1.54 \times 10^4$ M^{-1} cm^{-1}.

The plasmids pBR322, pBR322-3F3H (21), pPB520 (22), pMS421(23), pPB800 (22), pET15b-30 (24) and pGL10 (25) were isolated and purified using the QIAprep miniprep kit (Qiagen, USA). The pKD46 and pKD3 plasmids were obtained from the *E. coli* genetic stock center of Yale and Addgene respectively. The pPB800-TAAs and pGB^{nuc} vectors were constructed as described below.

Purification of proteins

6x His-tagged RecB^n (^{His}RecB^n) was purified as described (17). The plasmid for overexpression of RecB$^{1-927}$ and RecD was made by replacing bases 960–965 of pPB800 (26) with two TAA stop codons, and this plasmid is then transformed into a Δ*recCBD E. coli* strain V330 (19) carrying pPB520 (*recC⁺*) (26) and pMS421 (*lacI^q*) (23). This strain was grown, lysed, and RecB^{h}CD was purified chromatographically in the same way as wild-type RecBCD as described previously (27). We also generated two longer truncations of the RecB nuclease domain to generate RecB$^{1-866}$ and RecB$^{1-898}$. We expressed them together with RecC and RecD subunits as was done for the RecB$^{1-927}$ truncation. However, we failed to purify stable heterotrimeric RecBCD complexes with these longer deletions, despite clear expression of all the subunits.

Both RecB^{h}CD and ^{His}RecB^n are stored in buffer B (20 mM Tris–HCl, pH 7.5, 0.1 mM EDTA, 0.1 mM DTT, 100 mM
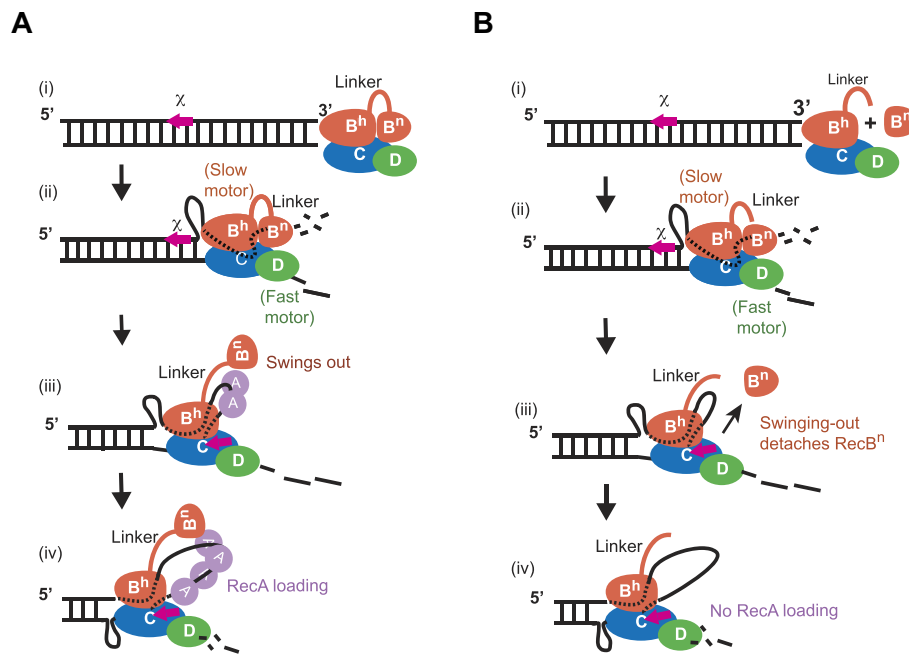
A   **B**

Figure 1. Illustration of the 'nuclease domain swing model' for RecBCD. (**A**) Upon recognition of the χ sequence, the nuclease domain is released to enable the subsequent loading of RecA onto a newly generated χ-containing ssDNA. (i) RecBCD binds to a duplex DNA end. (ii) The duplex DNA is unwound by the slow and fast motors (RecB and RecD respectively) of RecBCD. The nuclease domain preferentially degrades 3′-ended ssDNA-strand over the 5′-ended ssDNA-strand. The RecA-interacting region of the RecB nuclease domain is concealed through the interactions with the RecC subunit. (iii) χ recognition by RecBCD releases the RecB nuclease domain, revealing the RecA-interacting interface of RecB^n. RecA now interacts with RecB^n. (iv) RecBCD nucleates RecA onto the χ-containing ssDNA and the RecA–ssDNA filament grows. (**B**) Illustration of expected outcome of the nuclease swing model for an altered RecBCD with a severed tether. (i) RecB^{h}CD and RecB^n form a stable complex and the complex binds to a duplex DNA end. (ii) The RecB^{h}CD–RecB^n complex unwinds and degrades duplex DNA similar to wild-type RecBCD; the RecA-interacting interface of RecB^n is concealed. (iii) Upon recognition of χ, the interaction between RecB^{h}CD and RecB^n is reduced, causing RecB^n to detach and swing out from the rest of the enzyme. (iv) As a result, no loading of RecA onto χ-specific ssDNA is observed.

NaCl, 50% (v/v) glycerol at $-80°$C. RecB^{h}CD and ^{His}RecB^n have extinction coefficients of $\varepsilon_{280} = 4.2 \times 10^5$ and 4.6×10^4 M^{-1} cm^{-1} in buffer B, respectively. These values are determined by comparing the absorbance spectra of aliquots of protein in buffer B to spectra taken in 6 M guanidinium–HCl. The extinction coefficients of either RecB^{h}CD or ^{His}RecB^n in 6 M guanidinium–HCl at 280 nm was calculated from the amino acid sequence as described (28). RecA and SSB were purified as described (29).

Preparation of DNA substrates

DNA substrate χ^0 was prepared from circular plasmid pBR322, while χ$^+$ DNA was prepared from pBR322 3F3H, (a pBR322 derivative with two sets of three tandem χ-sequences) (21). These circular plasmid DNA were purified by cesium chloride density gradient centrifugation (30). The molar concentration of DNA was determined using an extinction coefficient of 6290 M^{-1} cm^{-1} nt^{-1} at 260 nm. Plasmid DNA was linearized using NdeI (NEB, Ipswich, MA) and radioactively labeled at the 5′-end by sequential reaction with shrimp alkaline phosphatase (USB Corp, Cleveland, OH) and T4 polynucleotide kinase (NEB, Ipswich, MA) and [γ-^{32}P] ATP (Perkin Elmer, Wellesley, MA) followed by purification with P30 BioSpin columns (Bio-Rad, Hercules, CA). 3′-labeling was performed by adding Klenow fragment (exo$^-$) of Polymerase I (NEB, Ipswich, MA) and [α-^{32}P] ATP (Perkin Elmer, Hopkinton, MA) to the linearized DNA and purified as described above.

Generation of ΔrecCBD strain of *E. coli* and plasmid constructions:

Generation of Δ*rec*CB*D*::FRT (flipase recognition target (FRT)) *AB1157* strain: For the generation of Δ*recCBD*::FRT AB1157 strain (31), the homologous regions of *recC* and *recD* genes (underlined), along with the chloramphenicol acetyltransferase gene (*cat*) of pKD3 plasmid was PCR amplified using the forward primer, 5′-GCTGGTGGAATATACCCATC AACTCGGGCAACCGCGCTGGCACCGCGCCAATCTCGT GTAGGCTGGAGCTGCTTC-3′ and reverse primer 5′-GAGCTTCCTCAAGCATCGCAATATAATCTTCGCCGCT CTGTAAAAGCCGTTTTTCGCATATGAATATCCTCCTT AG-3′. The purified PCR product was then transformed into a BW25113 strain carrying pKD46 plasmid (31). The P1 lysate of BW25113 transformants were later transduced into AB1157 cells. The *cat* gene was removed by FLP recombinase to obtain AB1157 Δ*recCBD*::FRT strain as described by Daysenko and Wanner method of one-step inactivation of genes in *E. coli* (31).

Construction of pPB800-TAAs: A 1.2 kb region of *recB* gene was PCR amplified using a forward primer 5′-CGCTGG CAACGCCTTATTAATCGACATCCAGCCG-3′ and a reverse primer 5′-CGGCTGGATGTCGATTAATAAGGCGT TGCCAGCG-3′ containing two stop codons at the 928th and 929th positions of *recB* gene. The PCR amplified region was digested with NcoI and SexAI enzymes and cloned into the NcoI and SexAI digested pPB800 vector (pKK223-3 based *recB* and *recD* overexpression plasmid (26)) to obtain pPB800-TAAs plasmid. The pPB800-TAAs contains two TAA

stop codons in the places of 928th and 929th amino acids of RecB. It expresses the $RecB^{1-927}$ and RecD polypeptides without $RecB^n$ domain. We also constructed vectors for expressing $RecB^{1-866}$ and $RecB^{1-898}$ truncated RecB proteins using following primers. RecB-866 forward primer – 5′-GTTTGC CAGGCAATTTATTAATCGCATAACGCTTC-3′ and RecB-866 reverse primer – 5′-GAAGCGTTATGCGATTAATAAA TTGCCTGGCAAAC-3′; RecB-898 forward primer-5′-CAAC GATTGCCCGGCTAATGATGGCGCGTCACCAGC-3′ and RecB-898 reverse primer 5′-GCTGGTGACGCGCCATCATT AGCCGGGCAATCGTTG-3′. The DNA sequencing was performed to confirm the integrity of the DNA sequence and presence of stop codons.

Construction of pGB^nuc: The XbaI–EcoRI restriction digested 1.2 kb DNA fragment containing $RecB^n$ gene from the pET-15b-30 vector (24) was cloned into a low copy number plasmid pGL10 vector (25) at the XbaI–EcoRI sites. DNA sequencing was performed to confirm the integrity and presence of $RecB^n$ gene, and expression of $RecB^n$ was also confirmed.

Protein–protein interaction assays using Ni-NTA magnetic beads

Ni-NTA magnetic beads (QIAGEN, Valencia, CA) were used to study the interactions between $^{His}RecB^n$ and $RecB^hCD$ as described (17). $RecB^n$ (0.5 μM) was incubated with various amounts of $RecB^hCD$ at the indicated conditions in 50 mM Tris–acetate pH 7.5, 50 mM NaCl, 50 mM imidazole, 0.2% Triton X-100 for 15 min. Ni-NTA beads were added to a final concentration of 1%, and the beads were immobilized, washed, and eluted as described (17). Eluted fractions were analyzed on 12% SDS-PAGE, followed by staining with Coomassie brilliant blue and quantified on a Gel Pro Analyzer (Media Cybernetics, Bethesda, MD). The amount of protein eluted was calculated by comparison to known quantities of each protein. The quantitative measurement was done by the densitometric analysis of Coomassie blue-stained protein bands. The binding isotherm was analyzed by assuming one $RecB^n$ binds to one $RecB^hCD$ as described in Scheme 1:
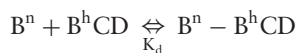
$$B^n + B^hCD \underset{K_d}{\Leftrightarrow} B^n - B^hCD$$

(Scheme 1)

where B^n represents $RecB^n$, and B^hCD stands for $RecB^hCD$. The dissociation constant K_d is defined in the equation (1):

$$K_d = \frac{[B^n]\,[B^hCD]}{[B^n - B^hCD]} \quad (1)$$

Since $RecB^hCD$ can only bind to the Ni-NTA beads when it forms a complex with the $^{His}RecB^n$, the amount of $RecB^hCD$ eluted from the Ni-NTA beads equals the amount of $RecB^hCD$–$RecB^n$ complex formed. The ratio of [$RecB^hCD$–$RecB^n$] to total [$RecB^n$] is given in equation (2):

$$\frac{\left[B^n - B^hCD\right]}{B^n_T}$$

$$= \frac{K_d\left(1 + B^n_T + B^hCD_T\right) - \sqrt{(K_d + B^n_T - B^hCD_T) + 4K_d \cdot B^hCD_T}}{2B^n_T}$$

(2)

where B^n_T and B^hCD_T stand for the total concentrations of $RecB^n$ and $RecB^hCD$, respectively. Data were analyzed by nonlinear least square (NLLS) analysis using Scientist (Micro-

math, St. Louis, MO) and equations (1) and (2) to determine K_d.

χ-specific ssDNA formation assay

χ-specific ssDNA formation assays were performed by mixing 10 μM (nts) radioactively labeled dsDNA, 0.1 nM RecBCD (or 0.1 nM $RecB^hCD$ plus 1 μM $RecB^n$) and 1 μM SSB in 25 mM Tris–acetate, pH 7.5, and 10 mM $Mg(OAc)_2$ unless noted otherwise. This mixture was incubated at 37°C for 3 min, and the reaction is initiated by addition of ATP to 5 mM. 10 μl aliquots were removed at each specified time points and quenched with 65 mM EDTA followed by deproteinization with 2% (w/v) SDS and 1 mg/ml proteinase K (Roche, Indianapolis, IN). These were loaded onto a 1% agarose gel and run at 40 V for 16 h. The gel was dried and exposed to a phosphor screen and quantified on a Storm PhosphorImager (GE Healthcare, Piscataway, NJ).

The fraction of χ-containing ssDNA produced $f_{Chi}(t)$ at time t was calculated using equation (3):

$$f_{Chi}(t) = \frac{\frac{c_{Chi}(t)}{c_{ds}(t)+c_{ss}(t)+c_{Chi}(t)} - \frac{c_{Chi}(0)}{c_{ds}(0)+c_{ss}(0)+c_{Chi}(0)}}{1 - \frac{c_{Chi}(0)}{c_{ds}(0)+c_{ss}(0)+c_{Chi}(0)}} \quad (3)$$

where $c_{Chi}(t)$, $c_{ds}(t)$ and $c_{ss}(t)$ are the counts of the bands corresponding to the χ-containing ssDNA, dsDNA and ssDNA at time t, respectively. Since DNA is in excess, all the $RecB^hCD$–$RecB^n$ complexes should be bound to dsDNA. Thus, the fraction χ-containing ssDNA produced should reflect the ratio of $RecB^hCD$–$RecB^n$ complexes formed to total [$RecB^hCD$]. This relationship can be expressed in terms of K_d, total [$RecB^n$] and [$RecB^hCD$] as given in equation (4):

$$f_{Chi}(t) = \frac{\left[RecB^n - RecB^hCD\right]}{[RecB^hCD]_{total}}$$

$$= \frac{K_d\left(1 + B^n_T + B^hCD_T\right) - \sqrt{(K_d + B^n_T - B^hCD_T) + 4K_d \cdot B^hCD_T}}{2 \cdot B^hCD_T}$$

(4)

Data were analyzed using NLLS with Scientist (Micromath, MO) to determine K_d.

χ-dependent reversible inactivation assay

χ-dependent reversible inactivation of DNA unwinding was performed as described (32). The reaction mixture was the same as the regular χ-specific ssDNA formation assay (25 mM Tris–acetate, 5 mM ATP, and 1 μM SSB monomers) except that the concentrations of RecBCD and $RecB^hCD$ were 0.1 and 0.2 nM, respectively, and the concentration of $Mg(OAc)_2$ was 1 mM. Assay temperature was at 37 °C, and 40 min after the reaction was initiated by addition of 5 mM ATP, excess $Mg(OAc)_2$ was added to a final concentration of 10 mM. Aliquots were removed at specified time points and processed as described above.

Joint molecule formation assay

Coupled joint molecule formation reactions for RecA–RecBCD, $RecB^hCD$ and $RecB^hCD$–$RecB^n$ were conducted as described earlier (7,12). Briefly, reactions were carried out in 25 mM Tris–acetate (pH 7.5), 8 mM $Mg(OAc)_2$, 5 mM ATP, 1 mM dithiothreitol, 1 mM phosphoenolpyruvate, 2 units/ml pyruvate kinase, 10 μM (nucleotides) 5′-end-labeled NdeI-linearized χ⁺-pBR322 3F3H dsDNA, 20 μM (nucleotides) su-

percoiled circular χ^+-pBR322 3F3H DNA, 5 μM RecA protein, 2 μM SSB protein and either 0.3 nM RecBCD, 0.9 nM RecB^{h}CD, or 0.3 nM RecB^{h}CD with 1 μM RecB^{nuc}. When the RecB^n concentration was varied as indicated, reactions contained 0.3 nM RecB^{h}CD. Reactions were terminated at indicated times by adding stop buffer. The reaction products were separated on a 1% (w/v) TAE (40 mM Tris–acetate (pH 8.2) and 1 mM EDTA) agarose gel at 600V·h, visualized, and quantified using Amersham Biosciences Storm 840 PhosphorImager and ImageQuant software.

UV sensitivity test

E. coli strain AB1157 $\Delta recCBD$::FRT containing pMS421 (for *lacI^q* expression) pPB520 (RecC expression), pPB800 (RecB and RecD expression), pPB800-TAAs (for RecB^{927} expression without RecB^n and RecD expression), and pGB^n (RecB^n expression on a low copy number plasmid pGL10) were gown overnight in LB broth containing spectinomycin (20 μg/ml), chloramphenicol (25 μg/ml), ampicillin (100 μg/ml) and kanamycin (30 μg/ml) antibiotics. An aliquot (50 μl) of an overnight culture was inoculated into 5 ml of LB medium and was allowed to grow till early log phase (OD$_{600}$ = 0.5) at 37°C. Serial dilutions of cells were made, and 5 μl of diluted cells were spotted on LB agar plates. The plates were irradiated with UV light (254 nm) using a Spectroline short wave UV lamp (model-XX-15F, Spectronics corporation, NY, USA) for 0, 4, 8 and 12 seconds at a UV dose of 0.3 J/m^2/s. The colonies that survived UV irradiation after incubation at 37°C for 20 h in the dark were scored.

T4 *2$^-$* plaque assay

E. coli strain AB1157 $\Delta recCBD$::*FRT* expressing RecBCD mutant enzymes from plasmids pPB520, pPB800, pPB800-TAAs and pGB^n were grown overnight in LB broth containing chloramphenicol (25 μg/ml), ampicillin (100 μg/ml) and kanamycin (30 μg/ml) as needed. The pPB800, pPB800-TAAs, pPB520 and pGB^n are the low-copy expression vectors having 10–20 copies per cell and these proteins were expressed under LacI^q repression (from the pMS421 plasmid) without IPTG induction. An aliquot (50 μl) of an overnight culture was inoculated into 5 ml of LB medium containing suitable antibiotics, was allowed to grow till early log phase (OD$_{600}$ = 0.5) at 37°C. Early log cell culture (0.1 ml) was mixed with 3 ml of LB top agar and spread on LB bottom agar plates. Plates were allowed to dry for 15 min. Serial dilutions of the phage stock (10^9 plaque forming units/ml) were made in suspension medium (50 mM Tris–HCl, pH 7.5, 100 mM NaCl, 1 mM MgSO$_4$, 0.01% gelatin), and 5 μl of each dilution was spotted on LB agar plate containing bacterial cells. These plates were incubated at 37°C overnight, and the number of countable plaques formed under lower dilution was counted. T4 or T4 *2$^-$* phage titers from strains expressing RecBCD and derivatives were divided by the titer from strain AB1157 $\Delta recCBD$::FRT with an efficiency of plating (EOP) about 3 × 10^{10}/ml.

Lambda recombination and χ activity assay

The bacteriophage λ crosses were performed between λ phage 1081, λ phage 1082, λ phage 1083, and λ phage 1084. Cross 1 was performed between phage 1081 × 1082, and cross 2 between phage 1083 × 1084 as depicted below.

The frequencies of J$^+$R$^+$ recombinants of the mixed λ phage crosses (cross 1 and cross 2) from the *recBCD* null strains expressing RecBCD mutant enzymes from pPB520, pPB800, pPB800-TAAs and pGB^n vectors determined by plating them on *E. coli* strain 594 (*sup^0*) for recombinants, also on strain C600 (*supE*) for the total phage titer. The χ activity in these crosses was determined by the method of Stahl and Stahl (33) using the equation, χ activity $= \sqrt{(t \div c)\text{ cross }1 \div (t \div c)\text{ cross }2}$, where $(t \div c)$ is the ratio of turbid (t) to clear (c) plaques from cross 1 or cross 2, among J$^+$R$^+$ recombinants as described (20).

Quantification and statistical analysis

Data are presented as mean ± standard error of the mean (SEM) or standard deviation (SD), unless otherwise stated. At least three independent experiments have been performed for each experiment. Data from the protein–protein interactions using Ni-NTA magnetic beads and the χ-specific ssDNA formation assays were analyzed by nonlinear least square (NLLS) analysis using Scientist software (Micromath, MO). The gels were quantified using Gel Pro Analyzer (Media Cybernetics, Bethesda, MD). Data from the χ-dependent reversible inactivation, and the joint molecule formation assays were quantified using Amersham Biosciences Storm 840 PhosphorImager and analyzed using the ImageQuant software (GE Healthcare, Piscataway, NJ). Graphs and image processing were done using the Prism 5.0 (GraphPad, USA) and ImageJ (nih.gov) software programs.

Results

RecB^{h}CD forms a complex with RecB^n

We generated and purified a mutant of RecBCD that lacks the nuclease domain of RecB, and we designate it as RecB^{h}CD. To test whether the nuclease domain of RecB (RecB^n) can interact with this truncation of RecBCD, we performed a pull-down assay with 6x His-tagged RecB^n (^{His}RecB^n) (17) and un-tagged RecB^{h}CD. Ni-NTA beads retain protein with the 6x His-tag and, therefore, any un-tagged protein co-eluting with His-tagged protein demonstrates an interaction between the two. As shown in Figure 2A, RecB^{h}CD co-elutes with ^{His}RecB^n from the Ni-NTA beads only in the presence of ^{His}RecB^n. These results show that a complex is formed between RecB^{h}CD and ^{His}RecB^n.

We next performed a pull-down assay with varying the concentrations of RecB^{h}CD to measure the affinity between RecB^{h}CD and ^{His}RecB^n. The ratio of eluted [RecB^{h}CD]/[RecB^n] is plotted as a function of the total [RecB^{h}CD] in Figure 2B, and the data were analyzed with a nonlinear least square (NLLS) algorithm. The analysis yields an apparent dissociation constant (K_d) of 1.1 ± 0.5 μM, and the stoichiometry reaches a plateau value at 0.95 moles RecB^{h}CD per mole RecB^n.

The RecB^{h}CD–RecB^n complex produces χ-specific ssDNA fragments

We next examined if this reconstituted complex of RecB^{h}CD and RecB^n (formed by mixing the purified RecB^{h}CD and an excess of purified RecB^n) is functional with regards to χ-recognition by studying whether it can generate χ-specific ssDNA fragments (7). The formation of χ-specific ssDNA fragments was assayed using a 4.4 kb linear dsDNA containing a
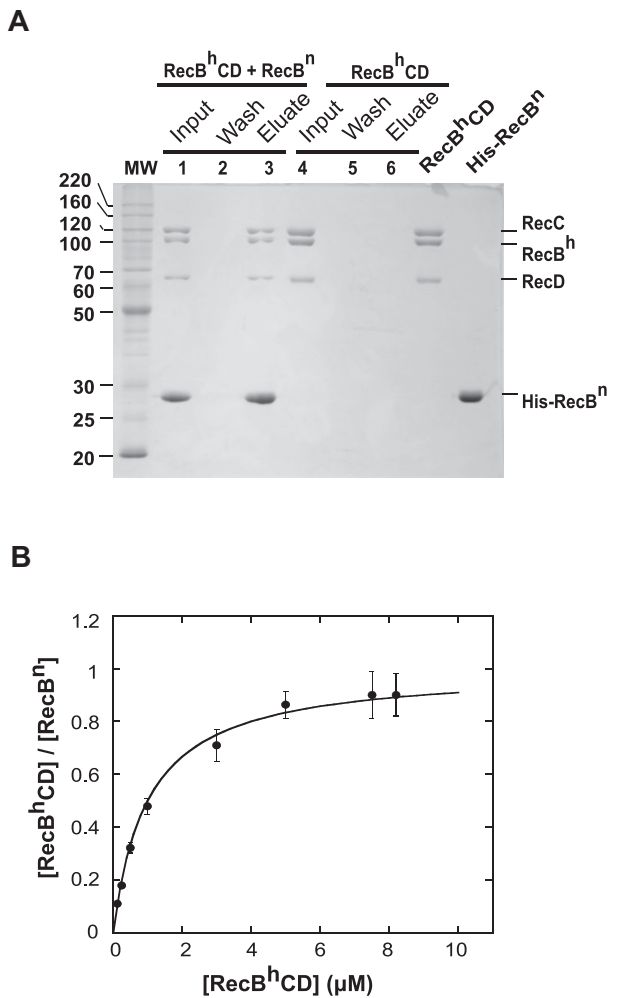
A

B

Figure 2. RecB^{h}CD forms a stable complex with RecB^n. The pull-down assay was performed using ^{His}RecB^n and RecB^{h}CD, as described in the Materials and Methods. (**A**) A representative pull-down experiment; incubation, wash and elution aliquots were analyzed using 12% SDS-PAGE. ^{His}RecB^n and RecB^{h}CD (1 μM each) were incubated with Ni-NTA beads, and an aliquot was removed at the end of incubation and loaded onto Lane 1. Lane 2 is the 3rd wash of the Ni-NTA beads with interaction buffer, and Lane 3 is the elution of Ni-NTA beads with 300 mM imidazole. A control was performed in the absence of ^{His}RecB^n by incubating Ni-NTA beads with RecB^{h}CD (2 μM), and the incubation, wash and elution aliquots were loaded onto Lanes 4, 5 and 6, respectively. The RecB^{h}CD and ^{His}RecB^n markers represent the equivalent of 2 and 1 μM, respectively. (**B**) Determining the binding affinity of RecB^{h}CD for RecB^n. Pull-down assays were performed with 0.5 μM ^{His}RecB^n and increasing amounts of RecB^{h}CD. The ratio of RecB^{h}CD to ^{His}RecB^n eluted from the bead was plotted as a function of total [RecB^{h}CD]. The solid line is a simulation using equation (2) and K_d of 1.1 ± 0.5 μM.

triple-χ sequence in each strand and labeled with ^{32}P at both 5′-ends (Figure 3A, top panel) (21). At a sub-stoichiometric amount of enzyme relative to DNA ends (0.1 nM of enzyme and 4.6 nM DNA ends), different χ-specific ssDNA fragments are produced by wild-type RecBCD depending on which DNA end is the entry site (Figure 3A, top panel). RecB^{h}CD alone can only unwind dsDNA to produce full-length ssDNA, and it does not degrade the ssDNA product despite an increased enzyme concentration (Figure 3B). Like RecBCD, the complex formed between RecB^{h}CD and RecB^n produced χ-specific ss-DNA when presented with χ$^+$ dsDNA (Figure 3A). Since
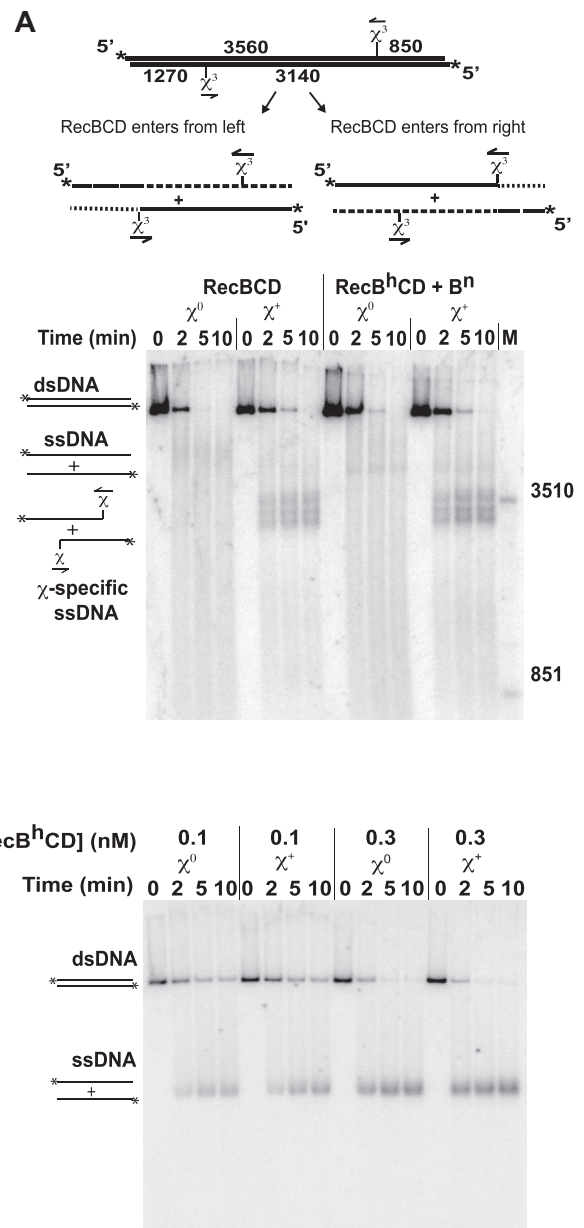
A

B

Figure 3. The reconstituted complex of RecB^{h}CD and RecB^n recognizes χ and produces χ-specific ssDNA fragments. (**A**) dsDNA (10 μM nt) with χ (χ$^+$) or without χ (χ^0) was reacted with either 0.1 nM RecBCD or 0.1 nM RecB^{h}CD plus 1 μM RecB^{nuc}. (**B**) dsDNA (10 μM nt), χ$^+$ or χ^0, was reacted with various concentrations of RecB^{h}CD. The location of the triple-χ sequence on the dsDNA is indicated in the inset and the asterisk (*) indicates the position of the γ^{32}P label. The additional fragment observed along with the expected χ-specific ssDNA fragments is likely due to dissimilar conformations of χ-containing ssDNA with different mobilities as was observed earlier (8,32).

RecB^n has a very low affinity for ssDNA (34), it is very unlikely that RecB^n is simply binding and digesting the unwound ssDNA products independently of RecB^{h}CD. If so, the location of such binding would be random, and therefore, a broad range of degraded ssDNA products should be produced instead of ssDNA products of a specific uniform length. Besides, RecB^n alone showed no degradation of linear dsDNA and ss-DNA substrates (see last two lanes of Figure 6A).
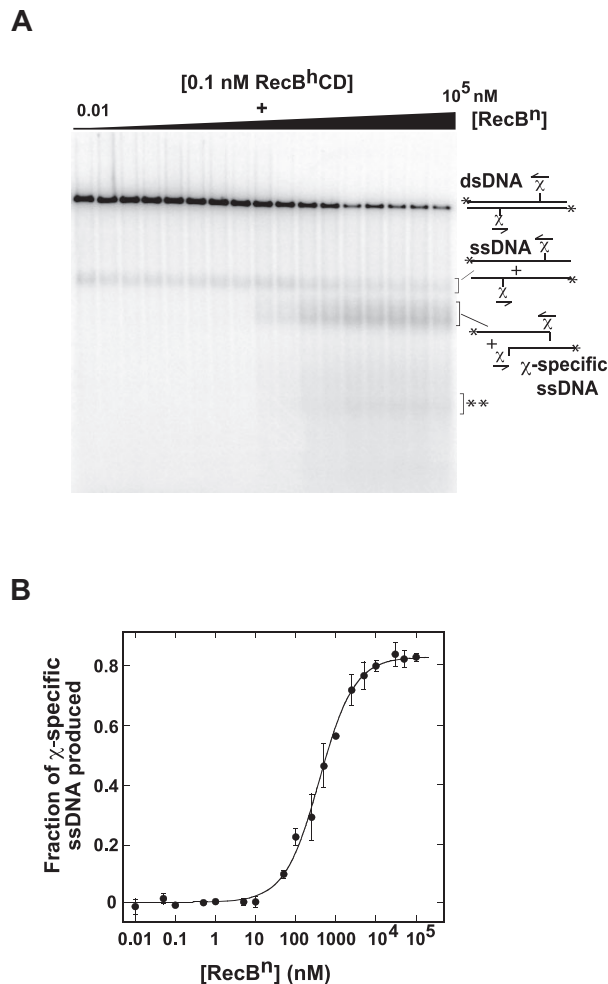
A

B

Figure 4. The affinity of RecB[n] for RecB[h]CD is increased in the presence of dsDNA and ATP. χ-specific ssDNA production was performed for 7 min at 37 °C with 0.1 nM RecB[h]CD, 20 μM (nt) χ+ DNA and varying amounts of RecB[n]. A representative experiment is shown in (**A**). The fraction of χ-specific ssDNA produced was quantified and plotted as a function of the total [RecB[n]] in (**B**). ** denotes the upstream χ-dependent fragments produced from the non-χ-containing DNA strand as described earlier (9,12). Data were analyzed (as described in the Materials and Methods) and yield an apparent K_d of 0.4 ± 0.1 μM. The solid line is a simulation using equation (4) and $K_d = 0.4$ μM.

The affinity of RecB[h]CD for RecB[n] increases in the presence of dsDNA and ATP

We next measured whether the binding affinity of RecB[h]CD for RecB[n] is affected by the presence of dsDNA and ATP. We measured χ-specific ssDNA production at varying concentrations of RecB[n] while holding the concentration of RecB[h]CD constant at 0.1 nM. Under the conditions where dsDNA ends are in large excess of RecB[h]CD, all RecB[h]CD as well as RecB[h]CD–RecB[n] complexes, are bound to the dsDNA ends. Therefore, the fraction of χ-containing fragments generated relative to the total amount of DNA equals to the ratio of RecB[h]CD–RecB[n] complex to RecB[h]CD bound at the ends of dsDNA. Thus, we can monitor the formation of the RecB[h]CD–RecB[n] complex as a function of [RecB[n]] and determine the binding affinity. Figure 4A shows a representative experiment. When the fraction of χ-specific ssDNA produced is plotted against total [RecB[n]], a K_d of 0.4 ± 0.1 μM is obtained from NLLS analyses of the data (Figure 4B). The affin-

ity for RecB[h]CD binding to RecB[n] is increased by ∼3-fold in the presence of dsDNA and ATP. Importantly, there is good agreement between the pull-down experiment and enzymatic assay.

RecB[h]CD recognizes χ despite failure to produce χ-specific fragments

We have shown RecB[h]CD alone cannot produce χ-specific ssDNA but can produce χ-specific ssDNA when it associates with RecB[n] (Figure 3A and B). This suggests that RecB[n] could play two possible roles within the reconstituted RecB[h]CD–RecB[n] complex. First, RecB[h]CD alone may not recognize the χ sequence but association with RecB[n] restores its ability to cleave the DNA up to the 3′-side of χ and then to recognize and attenuate at the χ site. Conversely, it is possible that RecB[h]CD intrinsically recognizes χ, but it cannot produce χ-specific ssDNA due to lack of nuclease activity. To distinguish between these two possibilities, we next examined whether RecB[h]CD can recognize χ or not.

Previous studies have established that the recognition of χ, under conditions of limiting free [Mg^{2+}], inhibits DNA unwinding by RecBCD (32). The time-course of unwinding reaches an apparent plateau at less than the total amount of dsDNA present. This apparent inhibition is reversed by the addition of excess Mg^{2+}, resulting in a burst of unwinding activity, and nearly complete dsDNA unwinding. This results in a distinctive biphasic time-course of unwinding, which is a characteristic behavior of χ-recognition. When χ is absent (χ^0), neither inhibition at low [Mg^{2+}] nor significant biphasic kinetics occur. We performed the same assay to determine whether RecB[h]CD exhibits the same χ-dependent reversible inhibition of dsDNA unwinding. The fraction of DNA unwound was obtained from quantification of gels, and the time courses are plotted in Figure 5. The amount of χ-containing DNA unwound by both RecBCD and RecB[h]CD in 1 mM Mg(OAc)$_2$ reaches the same apparent plateau at 40 min. However, upon addition of excess Mg^{2+} to a final concentration of 10 mM, the unwinding rate increased in both cases, indicating that both RecBCD and RecB[h]CD recognize the χ sequence. Thus, RecB[h]CD has the intrinsic capacity to recognize χ, and RecB[n] has no obligatory role in χ-recognition by the RecB[h]CD–RecB[n] complex; RecB[n] however is essential for nuclease activity and the related χ-specific ssDNA formation. This finding is in full agreement with earlier studies for RecBC, lacking RecD, enzyme (32).

The RecB[h]CD–RecB[n] complex facilitates χ-dependent RecA-loading

RecB[n] is essential for the RecA-loading process (16). So, although the reconstituted RecB[h]CD–RecB[n] complex produced χ-specific ssDNA fragments, whether it could load RecA onto that ssDNA needed to be determined. Consequently, we measured RecABCD-dependent joint molecule formation by RecBCD, RecB[h]CD, and RecB[h]CD–RecB[n] enzymes as described previously (7,12). The results show that formation of RecA-dependent, χ-dependent joint molecules (the faster migrating 'χ-specific' joint molecules in Figure 6a) by the RecB[h]CD–RecB[n] complex is similar to that of the wild-type RecBCD enzyme. In contrast, RecB[h]CD alone failed to produce χ-specific joint molecules and produced only χ-independent joint molecules (from the full-length ssDNA products of unwinding) at a slower rate as previously observed
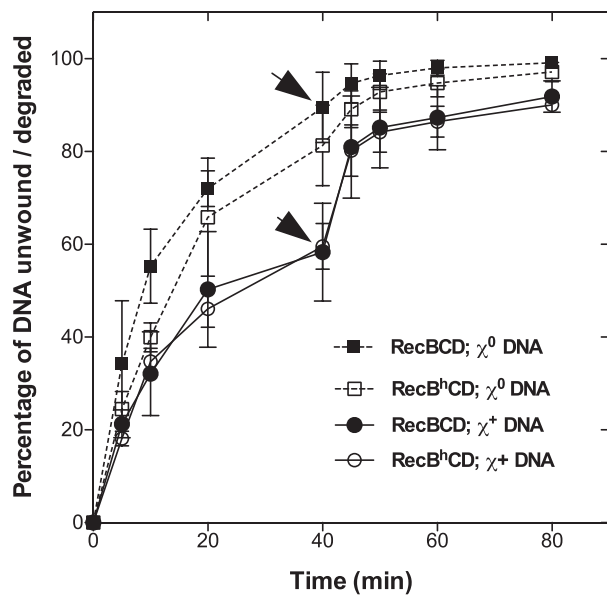
Figure 5. RecB^{h}CD recognizes χ as shown by reversible inactivation of dsDNA unwinding upon χ recognition. Either χ^0 or χ$^+$ DNA (10 μM nt) was reacted with 0.1 nM RecBCD or 0.2 nM RecB^{h}CD. Aliquots were removed at the times indicated, and excess Mg^{2+} was added after 40 min (indicated by arrows) to a final concentration of 10 mM. Comparison of the time courses of the fraction of DNA unwound by RecBCD with that of RecB^{h}CD is shown. Data are the mean ± SEM from two independent experiments.

([7,12]). The yields of χ-specific joint molecule formed after 10 minutes were 14.4 ± 1.4% and 13.4 ± 1.1% of the input linear dsDNA substrate for wild-type RecBCD and RecB^{h}CD–RecB^n enzymes, respectively (Figure 6B). RecB^{h}CD alone produced χ-independent joint molecules (4.0 ± 0.4% at 10 min); this slower rate is comparable to that of mutant RecBCD enzymes that lack RecA-loading function ([16,21]). Incubation of RecB^n domain alone with linear dsDNA or with ssDNA for 10 min showed no effect (Figure 6A, last two lanes). These findings affirm that the RecB^{h}CD–RecB^n complex is capable of loading RecA onto the χ-containing ssDNA, and importantly, that the covalent attachment—tethering—between the RecB helicase and RecB^n domains is not necessary for the RecA-loading process

The RecB^{h}CD–RecB^n complex is DNA repair and nuclease proficient *in vivo*

To corroborate our *in vitro* findings, we determined the *in vivo* proficiency of RecB^{h}CD–RecB^n with regards to its DNA repair function by measuring sensitivity to ultraviolet (UV) irradiation, and to its nuclease activity by measuring infectivity of T4 2^- phage. Cells expressing RecB^{h}CD–RecB^n, RecB^{h}CD, and wild-type RecBCD proteins on plasmids in a *recBCD* null strain were compared. As shown in Figure 7, cells expressing RecB^{h}CD protein alone are highly UV sensitive, comparable to the strain that lacks *recBCD* genes (Figure 7). Interestingly, co-expression of RecB^n and RecB^{h}CD proteins alleviated the UV sensitivity: the ability to repair the UV-induced DNA damage is comparable to the cells that are expressing wild-type RecBCD protein. This result suggests that the RecB nuclease domain is indeed capable of interacting *in trans* with RecB^{h}CD enzyme *in vivo* and protecting cells from UV-induced DNA damage.
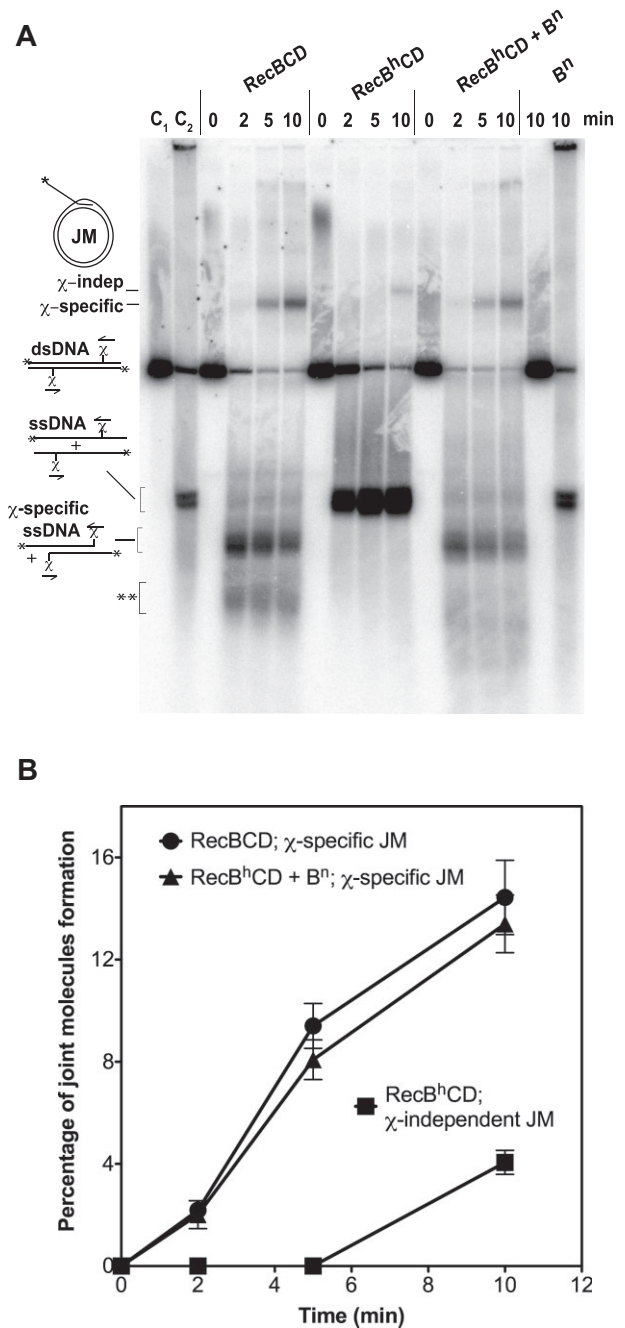

Figure 6. RecB^{h}CD–RecB^n loads RecA onto χ-containing ssDNA to form χ-specific joint molecule. (**A**) The χ-specific (χ-specific) and χ-independent (χ-indep) joint molecules (JM) formed, and the χ-specific ssDNA fragments produced as a function of time. C_1 and C_2 are control lanes with 5′-labeled linear dsDNA and ssDNA (heat-denatured dsDNA), respectively. The last two lanes are the reaction mixtures containing linear dsDNA and ssDNA with RecB^n alone. ** denotes the upstream χ-dependent fragments produced from the non-χ-containing DNA strand as described earlier ([9,12]). (**B**) Percentage of joint molecules formed relative to the input of linear dsDNA are plotted. Data points are the percentage of joint molecules formed by RecBCD (circles), RecB^{h}CD–RecB^n (triangles), and RecB^{h}CD (rectangles) proteins. Data are the mean ± SEM from three independent experiments.
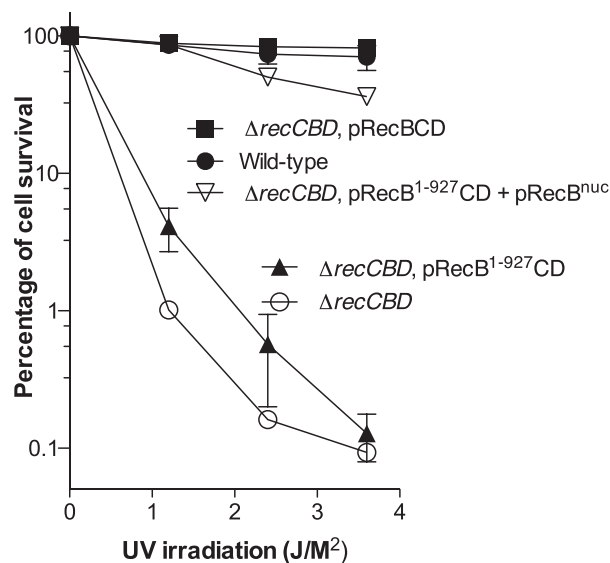
Figure 7. Co-expression of RecB^{h}CD and RecB^n proteins confers DNA repair proficiency to *E. coli* cells. A *recBCD* null strain expressing wild-type RecBCD, RecB^{h}CD, RecB^{h}CD–RecB^n proteins was subjected to UV irradiation. Percentage of cells surviving at various doses of UV irradiation are compared. Error bars of some data-points are minimal, hence not visible on the graph. Data are the mean ± SEM from the three independent experiments.

Table 1. Exonuclease activity of RecBCD mutants *in vivo*

E. coli strain	T4 phage titer[a]	T4 2− phage titer[a]
AB1157 (WT)	0.8 ± 0.1	1.8 ± 0.1 × 10^{-4}
ΔrecBCD::FRT	1	1
ΔrecBCD::FRT (pRecBCD)	1.0 ± 0.1	2.5 ± 0.3 × 10^{-4}
ΔrecBCD::FRT (pRecB$^{1-927}$CD)	2.0 ± 0.1	1.1 ± 0.1
ΔrecBCD::FRT (pRecB$^{1-927}$CD & pRecB^n)	0.8 ± 0.2	2.9 ± 1.7 × 10^{-3}

[a]Relative values: T4 wild-type or T4 *2−* phage titers from the indicated strains are divided by the titer on *ΔrecBCD::FRT* strain. Data are the mean ± SEM from three independent experiments.

If the RecB nuclease domain interacts with RecB^{h}CD *in vivo*, then it is expected to have nucleolytic activity. To determine whether the RecB^{h}CD–RecB^n complex has nucleolytic activity, we assayed T4 *2−* phage sensitivity. Wild-type T4 phage with a functional *gene 2* product is resistant to RecBCD-dependent DNA degradation due to the protection afforded by the binding of gene 2 protein to dsDNA ends of T4 phage DNA. However, T4 *2−* phages lacking gene 2 product make plaques only on the strain lacking RecBCD nuclease activity. Table 1 shows plaque formation by T4 *2−* in different backgrounds. In the strain expressing RecB^{h}CD and RecB^n proteins, viability T4 *2−* phage is decreased by almost a thousand-fold compared to the strain expressing RecB^{h}CD alone and is reduced only ∼10-fold compared to wild-type RecBCD. These results further confirm the ability of RecB^n to associate *in trans* with RecB^{h}CD *in vivo* to confer exonucleolytic activity to the cells.

Table 2. Recombination proficiency and χ activity of the RecBCD mutants *in vivo*

Strains	Cross 1 (1081 × 1082)	Cross 2 (1083 × 1084)	χ activity
AB1157 (WT)	8.7 ± 0.6	7.7 ± 0.6	5.1 ± 0.1
ΔrecBCD::FRT	0.1 ± 0.01	0.2 ± 0.05	1.1 ± 0.1
ΔrecBCD::FRT (pRecBCD)	8.7 ± 0.01	7.9 ± 0.3	5.7 ± 0.9
ΔrecBCD::FRT (pRecB$^{1-927}$CD)	0.9 ± 0.2	0.7 ± 0.4	1.5 ± 0.2
ΔrecBCD::FRT (pRecB$^{1-927}$CD & pRecB^n)	7.2 ± 0.7	6.9 ± 0.04	4.1 ± 0.3

Data are the mean ± SEM from two independent experiments.

The RecB^{h}CD–RecB^n complex promotes χ-stimulated homologous recombination *in vivo*.

We further investigated the functionality of the RecB^{h}CD–RecB^n complex in *vivo* by measuring χ-stimulated recombination between λ *red gam* phages which lack both the RecBCD-inhibiting Gam protein, and the λ recombination system, Red (33). Cells expressing RecB^{h}CD–RecB^n complex showed a ∼10-fold increase in λ recombinants and a ∼4-fold higher χ-stimulated crossover activity compared to the cells expressing RecB^{h}CD alone (Table 2); these values approach those of wild-type RecBCD. These results further confirm that the RecB^n indeed interacts with RecB^{h}CD *in vivo* to reconstitute a holoenzyme that is functional for χ-stimulated recombination in cells.

Discussion

RecBCD enzyme plays an essential role in the recombinational DNA repair of dsDNA breaks in *E. coli*. It is a multifunctional enzyme that initiates the DSB repair by nucleolytically processing the DSB. Its DNA resection activity serves as a prototype for dsDNA processing and mediator function in all organisms. Homologs or analogs specifically involved in resection exist in all organisms: in Eukaryotes, the Sgs1–Dna2–RPA–Top3–Rmi1 complex in *Saccharomyces cerevisiae* and the BLM–DNA2–RPA–TOP3α–RMI1–RMI2 complex in humans comprise functional analogs of the χ-activated RecBCD complex with regards to DNA resection (2,35–37).

RecBCD also possesses another essential activity: it mediates the delivery of RecA onto ssDNA that is complexed with SSB. This loading of RecA by RecBCD in response to χ-activation is a crucial step of recombinational dsDNA break repair; however, the detailed mechanism by which this occurs is not fully understood. RecBCD enzyme, specifically the nuclease/RecA-loading domain, is known to interact with RecA and to load RecA onto ssDNA, but only after recognition of χ. The isolated nuclease domain of RecB interacts directly with RecA and regions potentially responsible for such interactions were identified (17). Before recognition of χ, the RecA-interacting surface on RecB^n is occupied through the interactions with the RecC subunit (3). In response to χ, by an unspecified structural mechanism, the concealed RecA-interacting interface of RecB^n is revealed to facilitate RecA-loading onto ssDNA (12,16,17,38).

One model, the 'nuclease domain swing model', described in the Introduction, proposed that upon χ-recognition, conformational changes in RecBCD liberate RecB[n] from its binding site on RecC resulting in the exposure of the RecA-interacting surface of RecB[n]. The 70 aa linker was envisioned to tether the loading-domain in proximity to the newly generated ssDNA (Figure 1A(iii)). RecA then interacts with RecB[n] and is nucleated on the χ-containing ssDNA (Figure 1A(iv)) (4,14–17). A prediction of the simplest form of this model is that without a tether, if RecB[n] were to be released, none of the RecB[n]-dependent events downstream of χ-recognition would occur.

We examined this model by severing the link between RecB[h]CD and RecB[n]. We discovered that we could reconstitute the activities of wild-type RecBCD, despite the absence of a contiguous covalent linker. Pull-down experiments showed that the RecB[h]CD forms 1:1 complex with RecB[n] in the absence of DNA with an affinity, similar to that observed between RecA and RecB[n] ($K_d \sim 1$ μM) (17). In the presence of dsDNA and ATP, the affinity between RecB[h]CD and RecB[n] increases slightly ($K_d = 0.4 \pm 0.1$ μM). As is evident from the enzymatic assays and consistent with the equilibrium binding constant, RecB[h]CD is predominantly free and not bound to RecB[n] until concentrations greater than ~0.4 μM (e.g. see Figure 4), suggesting that a function of the linker is to ensure interaction of nuclease and RecA-loading domain with the RecBCD holoenzyme by creating a unimolecular species of RecB[h] and RecB[n].

Unexpectedly, we discovered that the reconstituted complex formed between RecB[h]CD and RecB[n] can process χ-containing dsDNA to produce χ-specific ssDNA as does wild-type RecBCD enzyme. Also, the reconstituted RecB[h]CD-RecB[n] complex is RecA-loading proficient like the wild-type RecBCD enzyme. Hence, the interactions between RecB[n] and RecB[h]CD are functional and sufficient for producing χ-specific ssDNA and RecA-loading. This conclusion is supported by *in vivo* observations of decreased plaque formation of T4 2^- phage in RecB[h]CD–RecB[n] expressing strain, showing that RecB[n] and RecB[h]CD form an active nuclease complex in cells. Furthermore, the RecB[h]CD–RecB[n] complex showed χ-dependent crossover hotpot activity in classical lambda phage crosses, confirming reconstitution of a functional RecBCD complex. These physiological measurements are slightly reduced compared to wild-type RecBCD, implying incomplete saturation of RecB[h]CD with RecB[n], again consistent with a function of the tether being to produce a single polypeptide comprising RecB[h]CD and RecB[n] rather than relying on bimolecular complex formation.

However, our findings that RecB[h]CD and RecB[n] can reconstitute typical RecBCD functions is in contradiction with the swing-model for RecA loading. Specifically, the results show that an intact covalent tether is unnecessary; thus, RecBCD has reorganized itself after χ-recognition and the RecA interaction site of RecB[n] was revealed without covalent tethering. Thus, in contrast to the prevailing model, non-covalent interactions between RecB[n] and RecB[h]CD play an important role in the association of RecB[n] with the rest of the enzyme even after recognition of χ. Based on our results, we propose that χ recognition causes conformational changes in both the RecB[n] and RecB[h]CD proteins. As a result, rather than swinging freely as a ball on a tether, RecB[n] functions while remaining attached to the rest of the enzyme but in a different conformation. These unexpected findings raise the question of what is the
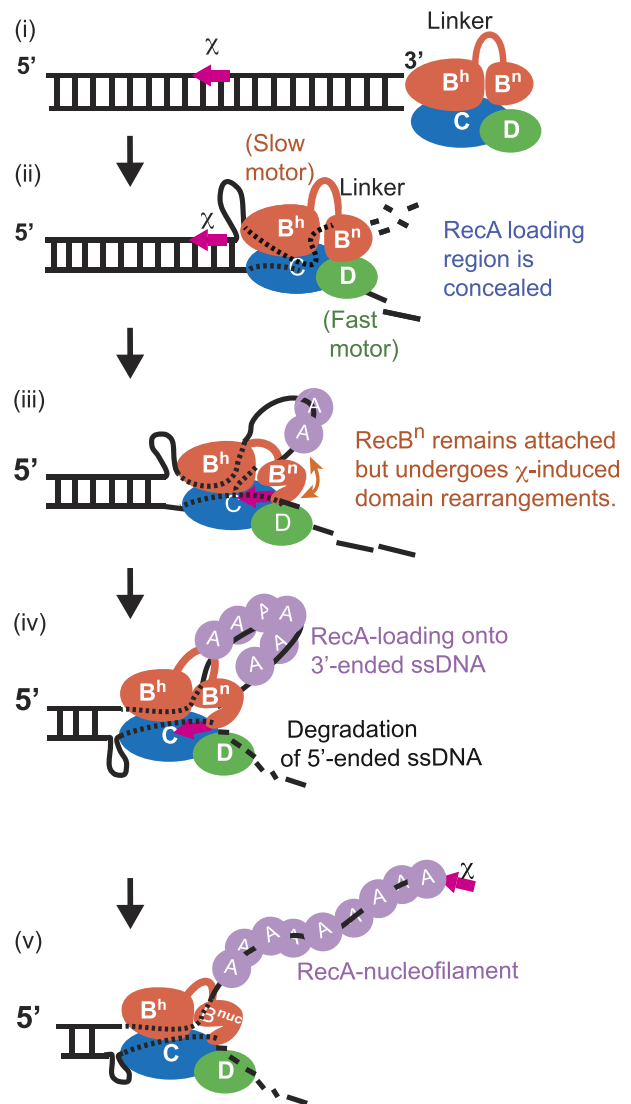

Figure 8. Model illustrating the prospective mechanism of χ-dependent RecA-loading by the RecBCD enzyme and double-strand break repair. (i) RecBCD binds to a duplex DNA end. (ii) The slow motor (RecB) and the fast motor (RecD) unwind duplex DNA. The differential translocation speed between two motor creates a loop ahead of slow RecB motor. The unwound duplex DNA is degraded by RecB nuclease domain, and the 3′-end ssDNA is preferentially degraded over the 5′-ended ssDNA. (iii) RecBCD recognizes the χ sequence, and χ remains transiently bound to the RecC subunit. The χ-induced conformational changes in RecBCD leads to domain rearrangements of RecB nuclease while remaining attached to the rest of the RecBCD enzyme. (iv) The structural rearrangements affecting RecB[n] cause attenuation of nuclease activity, leaving χ-containing ssDNA with the χ sequence at the 3′-end, and reveal the RecA-interacting interface to load RecA onto the χ-containing ssDNA. (v) After RecA nucleation, bidirectional growth of the RecA filament needed for the homology search ensues (39).

function of the 70-aa linker? Our attempts to purify truncated RecB proteins with shorter linkers (RecB[1–866] and RecB[1–898]) revealed that the RecBCD heterotrimer was unstable, suggesting that the linker is likely also a 'strap' that is important to the stability of the RecBC complex within the heterotrimer.

Consequently, we propose a new model of RecA-loading by RecBCD in response to χ. RecBCD unwinds and degrades the duplex DNA from the DNA end (Figure 8(i)). Before the recognition of χ, the RecB[n] remains associated with the RecC

subunit, and the RecA-loading surface is concealed (Figure 8(ii)). RecBCD recognizes χ and the recognition of χ induces conformational changes in RecBCD causing rearrangement of interactions with the RecA-loading domain, RecB^n (Figure 8(iii)). These structural rearrangements both reveal the RecA-interaction interface and modify the degradative focus of RecB^n to produce 3′-ended, χ-containing ssDNA and facilitate RecA-loading onto it (Figure 8(iv)).

Data availability

The data underlying this article are available in the article and in its online supplementary material.

Conflict of interest statement

None declared.

References

1. Kowalczykowski,S.C., Dixon,D.A., Eggleston,A.K., Lauder,S.D. and Rehrauer,W.M. (1994) Biochemistry of homologous recombination in *Escherichia coli*. *Microbiol. Rev.*, **58**, 401–465.
2. Kowalczykowski,S.C. (2015) An overview of the molecular mechanisms of recombinational DNA repair. *Cold Spring Harb. Perspect. Biol.*, **7**, a016410.
3. Singleton,M.R., Dillingham,M.S., Gaudier,M., Kowalczykowski,S.C. and Wigley,D.B. (2004) Crystal structure of RecBCD enzyme reveals a machine for processing DNA breaks. *Nature*, **432**, 187–193.
4. Dillingham,M.S. and Kowalczykowski,S.C. (2008) RecBCD enzyme and the repair of double-stranded DNA breaks. *Microbiol. Mol. Biol. Rev.*, **72**, 642–671.
5. Taylor,A. and Smith,G.R. (1980) Unwinding and rewinding of DNA by the RecBC enzyme. *Cell*, **22**, 447–457.
6. Pavankumar,T.L., Exell,J.C. and Kowalczykowski,S.C. (2016) Direct fluorescent imaging of translocation and unwinding by individual DNA helicases. *Methods Enzymol.*, **581**, 1–32.
7. Dixon,D.A. and Kowalczykowski,S.C. (1991) Homologous pairing in vitro stimulated by the recombination hotspot, Chi. *Cell*, **66**, 361–371.
8. Dixon,D.A. and Kowalczykowski,S.C. (1993) The recombination hotspot χ is a regulatory sequence that acts by attenuating the nuclease activity of the E. coli RecBCD enzyme. *Cell*, **73**, 87–96.
9. Dixon,D.A. and Kowalczykowski,S.C. (1995) Role of the *Escherichia coli* recombination hotspot, χ, in RecABCD-dependent homologous pairing. *J. Biol. Chem.*, **270**, 16360–16370.
10. Anderson,D.G. and Kowalczykowski,S.C. (1997) The recombination hot spot χ is a regulatory element that switches the polarity of DNA degradation by the RecBCD enzyme. *Genes Dev.*, **11**, 571–581.
11. Yang,L., Handa,N., Liu,B., Dillingham,M.S., Wigley,D.B. and Kowalczykowski,S.C. (2012) Alteration of χ recognition by RecBCD reveals a regulated molecular latch and suggests a channel-bypass mechanism for biological control. *Proc. Natl. Acad. Sci. U.S.A.*, **109**, 8907–8912.
12. Anderson,D.G. and Kowalczykowski,S.C. (1997) The translocating RecBCD enzyme stimulates recombination by directing RecA protein onto ssDNA in a χ-regulated manner. *Cell*, **90**, 77–86.
13. Forget,A.L. and Kowalczykowski,S.C. (2012) Single-molecule imaging of DNA pairing by RecA reveals a three-dimensional homology search. *Nature*, **482**, 423–427.
14. Yu,M., Souaya,J. and Julin,D.A. (1998) The 30-kDa C-terminal domain of the RecB protein is critical for the nuclease activity, but not the helicase activity, of the RecBCD enzyme from Escherichia coli. *Proc. Natl. Acad. Sci. U.S.A.*, **95**, 981–986.
15. Amundsen,S.K. and Smith,G.R. (2019) The RecB helicase-nuclease tether mediates Chi hotspot control of RecBCD enzyme. *Nucleic Acids Res.*, **47**, 197–209.
16. Churchill,J.J. and Kowalczykowski,S.C. (2000) Identification of the RecA protein-loading domain of RecBCD enzyme. *J. Mol. Biol.*, **297**, 537–542.
17. Spies,M. and Kowalczykowski,S.C. (2006) The RecA binding locus of RecBCD is a general domain for recruitment of DNA strand exchange proteins. *Mol. Cell*, **21**, 573–580.
18. Churchill,J.J., Anderson,D.G. and Kowalczykowski,S.C. (1999) The RecBC enzyme loads RecA protein onto ssDNA asymmetrically and independently of χ, resulting in constitutive recombination activation. *Genes Dev.*, **13**, 901–911.
19. Chaudhury,A.M. and Smith,G.R. (1984) A new class of *Escherichia coli recBC* mutants: implications for the role of RecBC enzyme in homologous recombination. *Proc. Natl. Acad. Sci. U.S.A.*, **81**, 7850–7854.
20. Schultz,D.W., Taylor,A.F. and Smith,G.R. (1983) *Escherichia coli* RecBC pseudorevertants lacking Chi recombinational hotspot activity. *J. Bacteriol.*, **155**, 664–680.
21. Anderson,D.G., Churchill,J.J. and Kowalczykowski,S.C. (1999) A single mutation, RecB$_{D1080A}$, eliminates RecA protein loading but not Chi recognition by RecBCD enzyme. *J. Biol. Chem.*, **274**, 27139–27144.
22. Emmerson,P.T. (1968) Recombination deficient mutants of *Escherichia coli* K12 that map between *thyA* and *argA*. *Genetics*, **60**, 19–30.
23. Heath,J.D. and Weinstock,G.M. (1991) Tandem duplications of the lac region of the Escherichia coli chromosome. *Biochimie*, **73**, 343–352.
24. Zhang,X.J. and Julin,D.A. (1999) Isolation and characterization of the C-terminal nuclease domain from the RecB protein of Escherichia coli. *Nucleic Acids Res.*, **27**, 4200–4207.
25. Pavankumar,T.L., Sinha,A.K. and Ray,M.K. (2010) All three subunits of RecBCD enzyme are essential for DNA repair and low-temperature growth in the antarctic Pseudomonas syringae Lz4W. *PLoS One*, **5**, e9412.
26. Boehmer,P.E. and Emmerson,P.T. (1991) Escherichia coli RecBCD enzyme: inducible overproduction and reconstitution of the ATP-dependent deoxyribonuclease from purified subunits. *Gene*, **102**, 1–6.
27. Bianco,P.R. and Kowalczykowski,S.C. (1997) The recombination hotspot Chi is recognized by the translocating RecBCD enzyme as

the single strand of DNA containing the sequence 5′-GCTGGTGG-3′. *Proc. Natl. Acad. Sci. U.S.A.*, **94**, 6706–6711.

28. Lohman,T.M., Chao,K., Green,J.M., Sage,S. and Runyon,G.T. (1989) Large-scale purification and characterization of the Escherichia coli rep gene product. *J. Biol. Chem.*, **264**, 10139–10147.

29. Harmon,F.G. and Kowalczykowski,S.C. (1998) RecQ helicase, in concert with RecA and SSB proteins, initiates and disrupts DNA recombination. *Genes Dev.*, **12**, 1134–1144.

30. Sambrook,J., Fritsch,E.F. and Maniatis,T. (1989) *Molecular Cloning: A Laboratory Manual, Second Edition*. Cold Spring Harbor Laboratory Press, Cold Spring Harbor, New York.

31. Datsenko,K.A. and Wanner,B.L. (2000) One-step inactivation of chromosomal genes in Escherichia coli K-12 using PCR products. *Proc. Natl. Acad. Sci. U.S.A.*, **97**, 6640–6645.

32. Dixon,D.A., Churchill,J.J. and Kowalczykowski,S.C. (1994) Reversible inactivation of the *Escherichia coli* RecBCD enzyme by the recombination hotspot χ *in vitro*: evidence for functional inactivation or loss of the RecD subunit. *Proc. Natl. Acad. Sci. U.S.A.*, **91**, 2980–2984.

33. Stahl,F.W. and Stahl,M.M. (1977) Recombination pathway specificity of Chi. *Genetics*, **86**, 715–725.

34. Yu,M., Souaya,J. and Julin,D.A. (1998) Identification of the nuclease active site in the multifunctional RecBCD enzyme by creation of a chimeric enzyme. *J. Mol. Biol.*, **283**, 797–808.

35. Symington,L.S. (2014) End resection at double-strand breaks: mechanism and regulation. *Cold Spring Harb. Perspect. Biol.*, **6**, a016436.

36. Nimonkar,A.V., Genschel,J., Kinoshita,E., Polaczek,P., Campbell,J.L., Wyman,C., Modrich,P. and Kowalczykowski,S.C. (2011) BLM-DNA2-RPA-MRN and EXO1-BLM-RPA-MRN constitute two DNA end resection machineries for human DNA break repair. *Genes Dev.*, **25**, 350–362.

37. Cejka,P., Cannavo,E., Polaczek,P., Masuda-Sasa,T., Pokharel,S., Campbell,J.L. and Kowalczykowski,S.C. (2010) DNA end resection by Dna2-Sgs1-RPA and its stimulation by Top3-Rmi1 and Mre11-Rad50-Xrs2. *Nature*, **467**, 112–116.

38. Amundsen,S.K., Taylor,A.F. and Smith,G.R. (2000) The RecD subunit of the Escherichia coli RecBCD enzyme inhibits RecA loading, homologous recombination, and DNA repair. *Proc. Natl. Acad. Sci. U.S.A.*, **97**, 7399–7404.

39. Bell,J.C., Plank,J.L., Dombrowski,C.C. and Kowalczykowski,S.C. (2012) Direct imaging of RecA nucleation and growth on single molecules of SSB-coated ssDNA. *Nature*, **491**, 274–278.